Materials Science & Engineering A 618 (2014) 9–15

Contents lists available at ScienceDirect

Materials Science & Engineering A

journal homepage: www.elsevier.com/locate/msea

Unusual Young's modulus behavior in ultrafine-grained and microcrystalline copper wires caused by texture changes during processing and annealing

P.P. Pal-Val [a,*], Yu.N. Loginov [b], S.L. Demakov [b], A.G. Illarionov [b], V.D. Natsik [a], L.N. Pal-Val [a], A.A. Davydenko [c], A.P. Rybalko [d]

[a] B.I. Verkin Institute for Low Temperature Physics and Engineering, National Academy of Sciences of Ukraine, Kharkov 61103, Ukraine
[b] The First President of Russia B.N. Yeltsin Ural Federal University, Ekaterinburg 620002, Russia
[c] A.A. Galkin Donetsk Physico-Technical Institute, National Academy of Sciences of Ukraine, Donetsk 83114, Ukraine
[d] S. Kuznets Kharkov National University of Economics, Kharkov 61166, Ukraine

ARTICLE INFO

Article history:
Received 19 May 2014
Received in revised form
25 August 2014
Accepted 26 August 2014
Available online 16 September 2014

Keywords:
Elastic properties
Young's modulus
Severe plastic deformation
Crystallographic texture
Annealing

ABSTRACT

Effect of annealing on the dynamic Young's modulus E of ultrafine-grained (UFG) and microcrystalline (MC) copper obtained by combined severe plastic deformation (SPD) including repeated hydrostatic extrusion and drawing (UFG copper) or only repeated drawing (MC copper) is investigated. It is established that the Young's modulus in the SPD-prepared UFG and MC samples exceeds that in the coarse-grained fully annealed (CGFA) samples by 10% to 20%. Subsequent isothermal annealing at elevated temperatures between 90 and 470 °C leads to a sharp decrease of the Young's modulus for annealing temperatures above 210 °C. After annealing at 410 °C, the value of E reaches its minimal value that is 35% lower than E in CGFA samples (total change in E is about 50% of the initial value). Further annealing at higher temperatures leads to some increase in the Young's modulus. It is shown that the unusual behavior of the Young's modulus is caused by the formation of the ⟨111⟩ axial drawing texture in the SPD-treated samples which is replaced by the ⟨001⟩ annealing texture during the post-SPD heat treatments.

© 2014 Elsevier B.V. All rights reserved.

1. Introduction

Use of the severe plastic deformation (SPD) techniques is the most accessible way of obtaining bulk ultrafine-grained (UFG) and nanostructured (NS) metals and alloys [1]. However, the wide industrial application of the SPD-processed materials is now restricted to a great extent due to various factors. Among them, it should be noted that being subjected to SPD processing, metals and alloys have non-equilibrium defect structures that cause time and thermal instability of functional and operating characteristics of these materials. Besides, different SPD methods lead to the formation of essentially different structural states in the processed materials, in particular, to the formation of textures, multimodal grain size distributions, significant internal stresses, etc. In turn, the real structure determines most of the technological and operational properties of highly fragmented metals such as their strength, plasticity, elastic properties, durability, corrosion resistance, etc. That is why the study of formation details of concrete SPD-induced microstructures, their stability and influence on macroscopic properties of UFG and NS metals and alloys seems to be an important problem of material science both from fundamental and engineering points of view.

The Young's modulus E is the important technological and structure-sensitive parameter that gives integral information on structural changes in the volume of the materials under investigation. Till now, the main attention of researchers has been concentrated on studying the behavior of the dynamic components of the Young's modulus caused by the relaxation processes in various subsystems of defect structures of materials [2–8]. It has allowed, in particular, to detect changes in parameters of dislocation structures upon ageing and annealing of UFG and NS materials [3–7], to investigate the diffusion mobility of impurity atoms and grain boundaries [5,6], to reveal the presence of glass-like 'phase' in NS metals [8], etc. At the same time, practically beyond the attention of researchers still remains the problem of influence of the structural features on the Young's modulus at different stages of preparation of the UFG and NS metals and alloys and also upon post-SPD treatments. Indeed, processed at high temperatures (for instance, by hot rolling or forging) and/or well annealed polycrystals are, as a rule, macroscopically quasi-isotropic as to their

* Corresponding author. Tel.: +380 57 3410913.
E-mail address: palval@ilt.kharkov.ua (P.P. Pal-Val).

http://dx.doi.org/10.1016/j.msea.2014.08.069
0921-5093/© 2014 Elsevier B.V. All rights reserved.

elastic properties. The occurrence of even a slight texture during cold working (e.g., rolling, drawing or hydrostatic extrusion) should lead in some cases to appreciable anisotropy of the Young's modulus due to the strong orientation dependence of elastic properties. The study of the behavior of the Young's modulus of UFG and NS metals and alloys may give some valuable information on structural changes during the preparation of materials and subsequent technological procedures.

In the present work, the influence of annealing on the dynamic Young's modulus of UFG copper samples prepared by the repeated hydrostatic extrusion procedure and drawing is investigated. Non-trivial behavior of the Young's modulus in comparison with corresponding results on the ECAP-processed UFG copper [7] is revealed. A comparative investigation on the samples of microcrystalline electrolytic tough pitch (ETP) copper has allowed us to establish that the anomalous behavior of elastic properties is mainly due to the formation of the ⟨111⟩ axial texture in the samples subjected to drawing and its subsequent transformation into the ⟨001⟩ axial texture during annealing at elevated temperatures.

2. Experimental procedures and materials

2.1. Sample preparation

2.1.1. Ultrafine-grained FRTP copper

Samples of the UFG Fire Refined Tough Pitch (FRTP) copper were obtained using the combined severe plastic deformation (SPD) treatment that involved repeated hot extrusion, cold hydrostatic extrusion (HE), intermediate 30 min annealing at 150 °C and final drawing (D). The technological schedule of the sample preparation operations is presented in Table 1. Total reduction in the initial billet cross-section was 99.89% that corresponds to the cumulative deformation $e=6.77$. The average grain size was $d\sim200-300$ nm.

2.1.2. Microcrystalline ETP copper

Samples of the Electrolytic Tough Pitch (ETP) copper were passed through standard stages of industrial processing. At first, the rods 8 mm in diameter were obtained using hot rolling at a deformation rate of 334 s^{-1} and processing temperature of 610 °C. The average grain size was about 18 μm. The grains were equiaxed and a crystallographic texture in the hot-rolled samples was practically absent. Then the rods underwent repeated drawing down to the wire diameters of 2.39 mm and 1.38 mm. Thus, the cumulative relative reductions were 91% and 97%, and the logarithmic deformations were $e=2.416$ and $e=3.515$, respectively.

Table 1
Technological schedule of the ultrafine-grained fire refined tough pitch (UFG FRTP) copper sample preparation.

№/№	Operation	Diameter, (mm)	Reduction, (%)	e
1.	Initial billet	59	–	–
2.	Hot extrusion	43	46.88	0.633
3.		28	77.48	1.491
4.		22.5	85.46	1.928
5.	Ageing at 20 °C, 10 months	22.5	85.46	1.928
6.	Hot extrusion	18.8	89.85	2.287
7.	Cold hydrostatic extrusion	13	95.15	3.025
8.	Annealing at 150 °C, 30 min.	13	95.15	3.025
9.	Cold hydrostatic extrusion	10	97.13	3.550
10.		8	98.16	3.996
11.		6	98.97	4.572
12.		4	99.54	5.382
13.	Drawing	2	99.89	6.769

2.2. Young's modulus measurements.

Measurements of the Young's moduli were carried out by both dynamic and quasi-static techniques. High-frequency dynamic Young's modulus measurements in the UFG FRTP copper were carried out using the two-component composite oscillator [9]. Longitudinal standing waves were excited in the samples 25 mm in length and 2 mm in diameter at frequencies $f\approx70$ kHz by means of a piezoelectric transducer. The ultrasound wave vector coincided with the direction of hydrostatic extrusion and drawing. Temperature dependences of the dynamic Young's modulus $E(T)$ were measured in the temperature interval of $5-310$ K at constant ultrasonic strain amplitude $\varepsilon_o\sim1\times10^{-7}$ in the amplitude independent range. The cooling–heating rate was about 1 K/min.

Values of the quasi-static Young's modulus of the hot rolled ETP copper rods were obtained from the microhardness measurements at room temperature using the Oliver–Pharr method. The measurements were carried out on MHTX CSM Instruments device at a load of 1 N and loading rate of 50 μ/min.

To determine the low-frequency dynamic Young's modulus of the ETP copper, the dynamic mechanical analyzer DMA 242C Netzsch was used. Samples were dynamically loaded using a three-point bending scheme with a frequency of 1 Hz and a vibration strain amplitude of $\varepsilon_o\sim8\times10^{-5}$. The measurements were carried out in the temperature interval of $20-270$ °C in air.

2.3. Annealing of the samples

2.3.1. UFG FRTP copper

At first, the measurements on UFG FRTP copper were carried out on the as-prepared samples. Then the measurements were repeated after several 30 min isothermal annealings in vacuum at elevated annealing temperatures T_{ann} in the interval from 90 to 470 °C with a step of 20 °C. When the rate of the Young's modulus changes dE/dT_{ann} sharply increased, the temperature steps were reduced down to 10 °C. As it was done in [7], the interval of annealing temperatures was first chosen in such a way that the expected temperature of the primary recrystallization of severely deformed copper $T_R\approx135$ °C lay in the middle of this interval. However, the behavior of the Young's modulus in the annealed samples prepared using hydrostatic extrusion and drawing was cardinally different from that in the ECAP-processed copper. That is why the interval of T_{ann} was extended towards appreciably higher temperatures.

2.3.2. MC ETP copper

Wires 1.38 mm in diameter were annealed at temperatures T_{ann} from 300 to 550 °C with a step of 50 °C using controllable heating and cooling in the inductor of a high-speed quenching dilatometer RITA Linseis with a heating–cooling rate of 100 °C/s. High speed was chosen to reproduce conditions of industrial wire drawing combined with high-speed thermal processing.

3. Results

3.1. Ultrafine-grained FRTP copper

Temperature dependences of the dynamic Young's modulus of deformed and annealed samples are shown in Fig. 1 (for clarity, some intermediate dependences are not shown there). For comparison, dependences $E(T)$ obtained on coarse-grained fully annealed (curve CGFA) [10] and ECAP-processed (curve ECAP-4) [7] copper are cited in Fig. 1 as well. In contrast to the ECAP-processed samples, the values of the Young's modulus of the samples deformed by hydrostatic extrusion and drawing appeared to be more than 20% higher

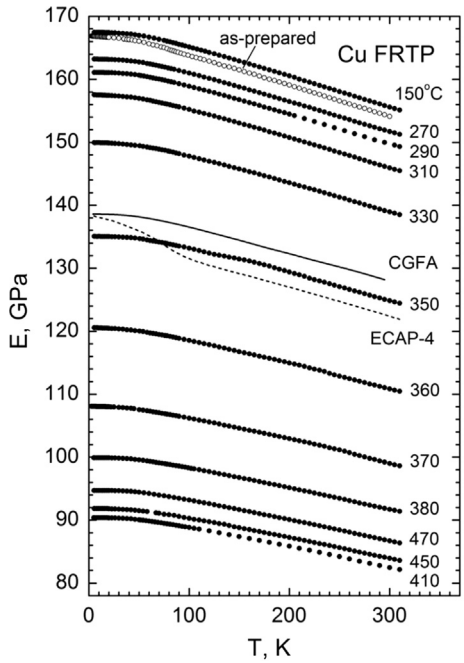

Fig. 1. Temperature dependences of the dynamic Young's modulus $E(T)$ in the ultrafine-grained fire refined tough pitch (UFG FRTP) copper samples measured at frequencies $f\sim70$ kHz: (○) – as-prepared; (•) – after isothermal annealing at elevated temperatures; annealing temperatures are indicated close to the curves. ECAP-4 – $E(T)$ in the UFG copper obtained by four ECAP runs [7]; CGFA – $E(T)$ in the coarse-grained fully annealed copper [10].

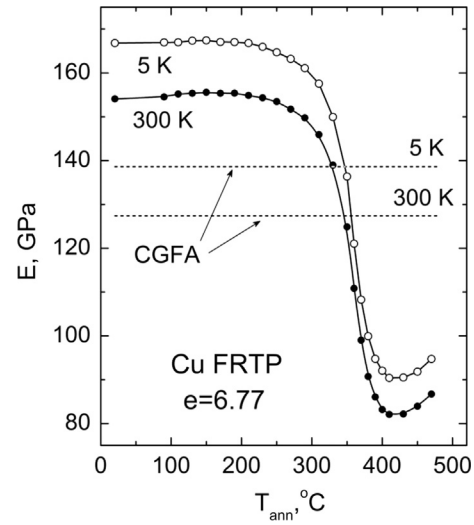

Fig. 2. Effect of annealing temperature on the dynamic Young's modulus at 5 K and 300 K in the ultrafine-grained fire refined tough pitch (UFG FRTP) copper. Dotted lines indicate the values of the Young's modulus in the coarse-grained fully annealed (CGFA) copper at these temperatures [7,10].

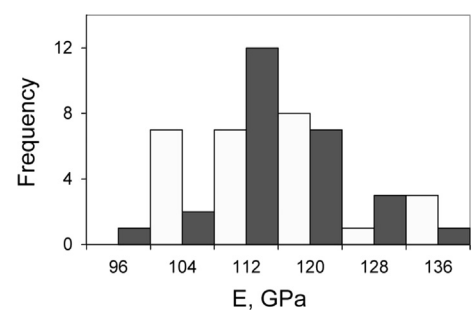

Fig. 3. Histogram of the Young's modulus variations in the microcrystalline electrolytic tough pitch (MC ETP) copper rods after hot rolling; dark and light bars are the values measured in two orthogonal directions on the sample cross-section. Values of the quasi-static Young's modulus were obtained from the microhardness measurements at room temperature using the Oliver–Pharr method.

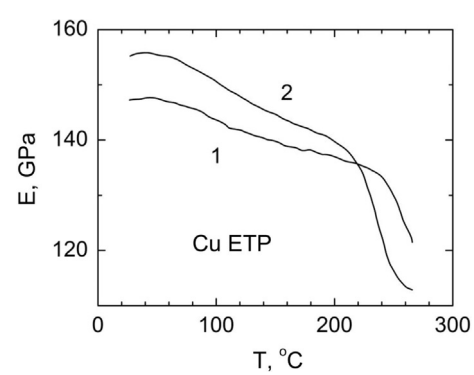

Fig. 4. Temperature dependences of the Young's modulus of the microcrystalline electrolytic tough pitch (MC ETP) copper drawn up to the plastic deformation e: 1–e=2.41; 2–e=3.51. The low-frequency dynamic Young's modulus was measured at a frequency of 1 Hz using the dynamic mechanical analyzer DMA 242C Netzsch.

than the corresponding values of E in the CGFA samples. Isothermal annealing at elevated temperatures led to the non-monotonic changes in the Young's modulus. Up to the annealing temperatures $T_{ann}=150$ °C, the Young's modulus increased over the whole investigated temperature range. At further increasing of T_{ann}, the Young's modulus values began to decrease, at first, rather slowly. Then the rate of the Young's modulus drop dE/dT_{ann} increased sharply and finally the entire dependence $E(T)$ appeared to be essentially below the curve obtained on the CGFA samples. The maximum rate of the Young's modulus changes $dE/dT_{ann}=1.4$ GPa/K was reached at $T_{ann}=360$ °C. The total reduction of the Young's modulus from its maximum down to minimum values amounted to 47% (see Fig. 2).

3.2. Microcrystalline ETP copper

The Young's modulus of the MC ETP copper rods processed according to a standard industrial hot rolling procedure had a noticeable dispersion of the values E measured at room temperature in different directions of the cross-sectional area 8 mm in diameter (see corresponding histograms in Fig. 3). It can be seen in Fig. 3 that the maximum of the distribution is located at $E=112$ GPa. This value is close to the lowest border of the Young's modulus estimation made for the quasi-isotropic copper polycrystals (more details are given below).

After cold drawing, the Young's modulus of the MC ETP copper increased from 112 GPa up to 147 GPa at a relative reduction of 91% ($e=2.41$) and 158 GPa at a relative reduction of 97% ($e=3.51$) (see Fig. 4). When increasing temperature, three stages of the Young's modulus changes may be distinguished. At first, a small increase in E occurred, then a smooth reduction of E was observed. At the third stage, the reduction of the Young's modulus sharply accelerated and reached the maximum rate at 235 °C ($e=3.51$) and 265 °C ($e=2.41$). The maximum rate of the Young's modulus change in the UFG FRTP copper ($e=6.77$) was reached at $T_{ann}=360$ °C (see Fig. 2).

It should be noted that the main result on the influence of the post-IPD heat treatment on the Young's modulus is obtained for UFG FRTP copper at relatively high frequencies $f\sim70$ kHz (Figs. 1 and 2). Another two sets of measurements were carried out on MC ETP copper using either quasi-static or low-frequency ($f\sim1$ Hz) techniques. They clearly demonstrate (a) a scatter of values of E in the rods when using the standard industrial hot rolling technique (Fig. 3) and (b) the qualitative similarity of the

Young's modulus behavior during heating of UFG FRTP and MC ETP samples (compare Figs. 2 and 4). As to the absolute values of the Young's modulus, we can compare those at 295 K for all the cases represented in Figs. 1–4. The lowest value $E=112$ GPa is obtained for coarse-grained MC ETP copper rods by the quasi-static micro-indentation method ($f\rightarrow 0$). In the coarse-grained fully annealed copper, $E=127.7$ GPa ($f\approx 70$ kHz) [7] and $E=128.2$ GPa ($f\approx 10$ MHz) [10]. In the SPD-processed MC ETP samples, $E=155.2$ GPa ($e=3.51$, $f\approx 1$ Hz) and in the UFG FRTP samples, $E=154.09$ GPa ($e=6.77$, $f\approx 70$ kHz). The absence of a significant and regular dependence of the dynamic Young's modulus on the measurement frequency testifies that in the samples investigated no pronounced relaxation processes of any nature are observed, at least in the vicinity of 295 K.

3.3. Texture analysis of the microcrystalline ETP copper

3.3.1. Stage of the accumulation of deformation

Drawing the wire causes non-uniform distributions of stresses and deformations and affects strongly their structure and mechanical properties. The angle of the drawing die and the friction boundary conditions are the important factors influencing the properties of the samples [11,12]. In particular, both parameters determine the texture in the peripheral and central parts of the deformed Cu samples.

To analyze the texture of the samples, the pole figures (PF) and inverse pole figures (IPF) were investigated in various cross sections of the wire. In Fig. 5, the inverse pole figures are shown for the dimensionless radial coordinate $r/R=0.86$ (r is the distance from the axis and R is the wire radius). It is established that at any relative coordinate, the direction ⟨111⟩ is the preferential orientation. The next in intensity, the ⟨001⟩ orientation, is characterized by a pole density from 2 to 3 times lower in the center of the wire and from 3 to 4 times lower in the peripheral layers of the wire in comparison with the ⟨111⟩ orientation. For their comparison, the pole densities I_p of the dominating ⟨111⟩ and ⟨001⟩ orientations are presented in Fig. 6. In more detail, an influence of the deflected mode on a zone representation of the textural components is described in [13].

3.3.2. Effect of thermal treatments

The EBSD maps of crystal grains orientations in the wire cross-section at various stages of preparation and subsequent annealing of the samples are shown in Fig. 7. The quantitative analysis shows that the average grain size diminishes from 18 μ in the hot rolled rods to 5 μ in wires after cold drawing (compare Fig. 7a and b, respectively) and then increases from 5 μ to 12 μ when annealing the samples (Fig. 7c,d). Besides, the replacement of the ⟨111⟩ orientation by the ⟨100⟩ orientation due to annealing is seen. Quantitatively the last process is characterized by diagrams in Fig. 8a and b. In the central zone (at rather small values r/R), the dominating ⟨111⟩ orientation in the hard-drawn sample (Fig. 8a) is replaced with ⟨001⟩ one after annealing (Fig. 8b). In the peripheral zone, a wide spectrum of the other orientations is observed. Prevalence of the ⟨001⟩ orientation in annealed wires causes much lower values of the Young's modulus than those in the quasi-isotropic polycrystalline copper.

4. Discussion

4.1. Abnormal changes in the Young's modulus value

Usually, intensive plastic deformation leads to essential (up to 10%) reduction in the Young's modulus of UFG metals [2–7]. In particular, that was established in experiments on the ECAP-deformed copper samples [3,5–7] (the ECAP-4 curve in Fig. 1 is taken from [7]). It was shown that the Young's modulus decrease observed in the ECAP-deformed copper is, mainly, due to a considerable increase of the dislocation density giving a large dislocation contribution to the elastic deformation. The dislocation nature of the dynamic Young's modulus reduction was proved when studying the Bordoni acoustic relaxation in ECAP-processed copper below and above the temperature of the Bordoni relaxation peak $T_B\approx 80$ K [7]. The maximum reduction of the Young's modulus (a modulus defect) was observed at $T>T_B$. In the low temperature range ($T\rightarrow 5$ K), the relaxation process caused by the thermally activated kink pair formation on dislocations is 'frozen,' and the reduction of the Young's modulus is minimized as it can be seen in Fig. 1 (for details see [6,7]). Subsequent annealing of the ECAP-4 samples at elevated temperatures led to a significant reduction of the dislocation density, the decrease of the dislocation-related anelastic strain component and the corresponding increase of the effective Young's modulus. The Young's modulus temperature dependences of the ECAP-4 samples approached the CGFA dependence up to almost full coincidence with that after annealing at $T_{ann}>150$ °C.

An entirely different behavior has been observed in the present work. Immediately after the SPD-processing, unexpectedly high values of the Young's modulus were registered and their subsequent huge reduction at high-temperature annealing was revealed.

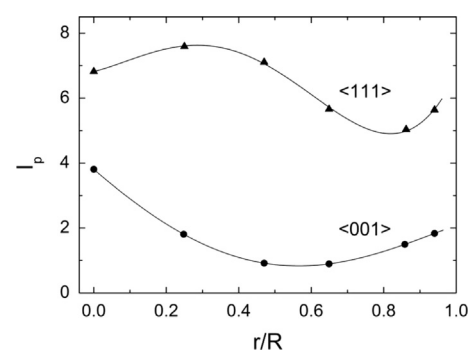

Fig. 6. Pole densities of the dominating ⟨111⟩ and ⟨100⟩ orientations along the drawing direction versus relative radial coordinate in the microcrystalline electrolytic tough pitch (MC ETP) copper.

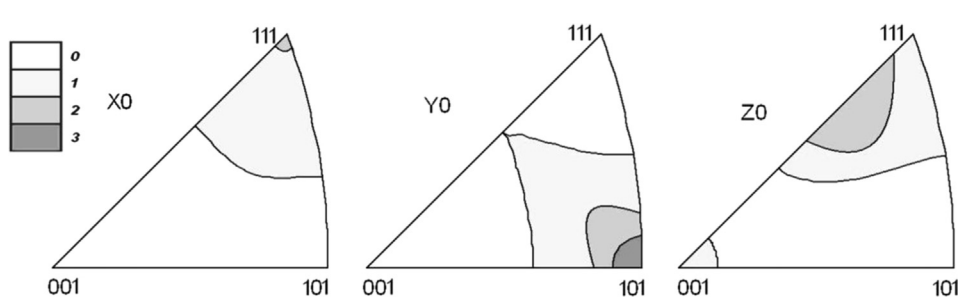

Fig. 5. Inverse pole figures of the microcrystalline electrolytic tough pitch (MC ETP) copper wire cross-section at the relative radial coordinate $r/R=0.86$. XO and YO are the radial and tangential directions, respectively, ZO is the direction of drawing.

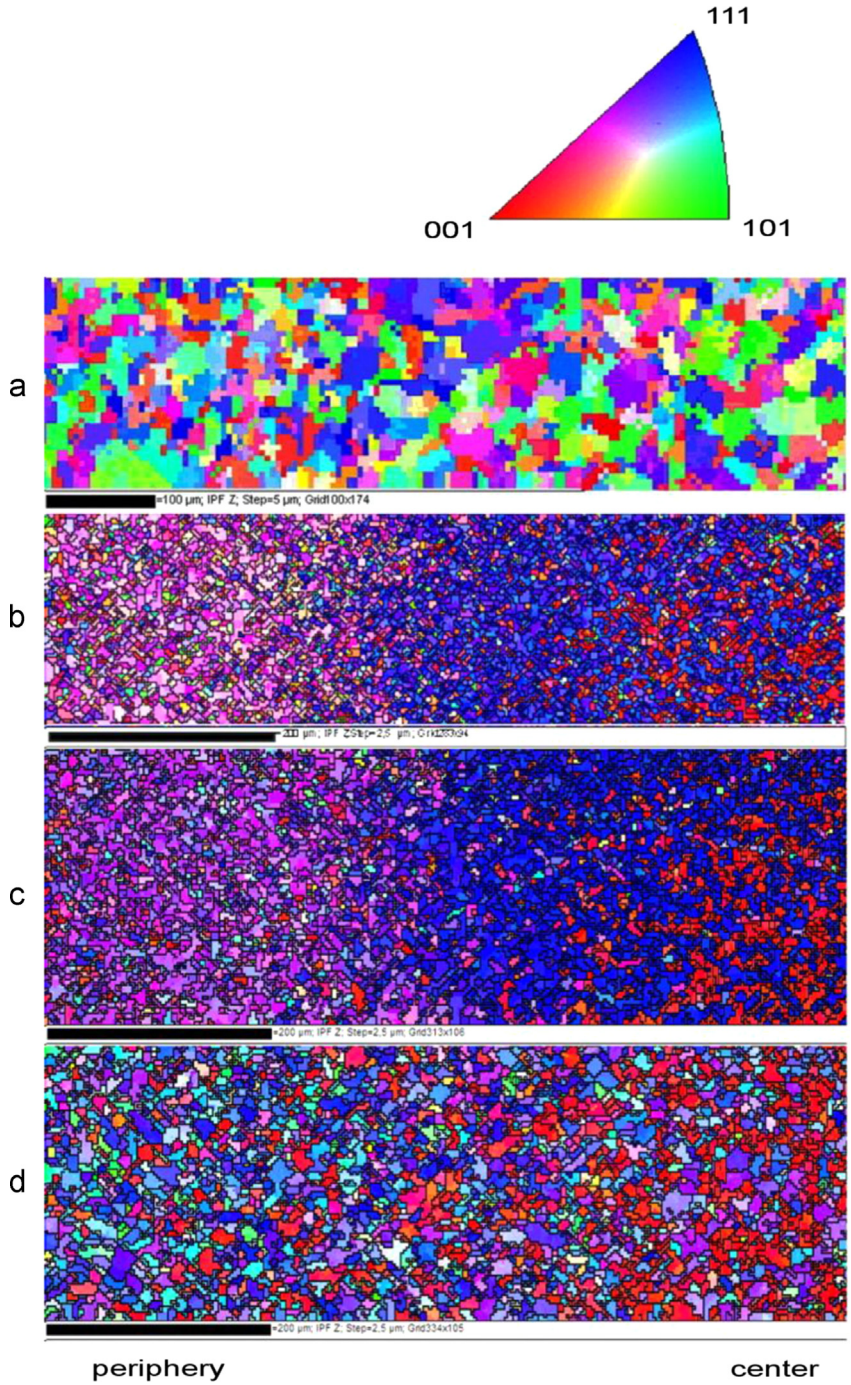

Fig. 7. EBSD orientation maps of the microcrystalline electrolytic tough pitch (MC ETP) copper texture distribution at the main stages of sample preparation and subsequent annealing: (a) after hot rolling; (b) after hard drawing; (c) after annealing at 300 °C; and (d) after annealing at 500 °C. The center of a sample is located at the right side of the figure, and the peripheral area is at the left one.

To explain these experimental results, let us consider, first, the problem of possible limits of the Young's modulus variation in the crystalline copper. As it is well known [14], the orientation dependence of the Young's modulus of the crystals with cubic symmetry can be expressed as

$$E^{\langle hkl\rangle} = \left[\frac{(C_{11}+C_{12})}{(C_{11}+2C_{12})(C_{11}-C_{12})} + r\left(\frac{1}{C_{44}} - \frac{2}{C_{11}-C_{12}}\right)\right]^{-1}, \quad (1)$$

where C_{11}, C_{12} and C_{44} are the components of the elastic stiffness tensor, $r = l_{11}^2 l_{12}^2 + l_{11}^2 l_{13}^2 + l_{12}^2 l_{13}^2$, and l_{ij} are the direction cosines. The Young's modulus has extrema for the crystallographic directions ⟨001⟩ and ⟨111⟩. The sections of the characteristic Young's modulus surfaces for copper by the $(1\bar{1}0)$ plane are presented in Fig. 9. The plot shows that the Young's modulus has the maximum in the direction ⟨111⟩ and the minimum in the direction ⟨001⟩: $E^{\langle 111\rangle}=205.0$ and 191.4 GPa, $E^{\langle 001\rangle}=73.2$ and 67.0 GPa at 5 and 300 K, respectively. Thus, the values of E obtained in our experiment appear to be within the possible limits of the Young's modulus in copper single crystal.

4.2. Young's modulus of polycrystals

If a single-phase polycrystalline sample consists of sufficiently large number of grains (in other words, the average grain size is

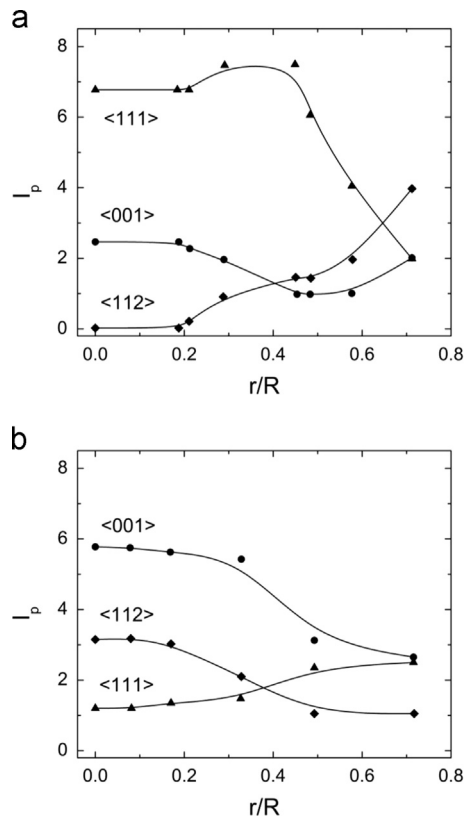

Fig. 8. Intensities of the ⟨111⟩, ⟨001⟩ and ⟨112⟩ textures of the microcrystalline electrolytic tough pitch (MC ETP) copper as a function of the relative radial coordinate (a) in the deformed state and (b) after annealing at 500 °C.

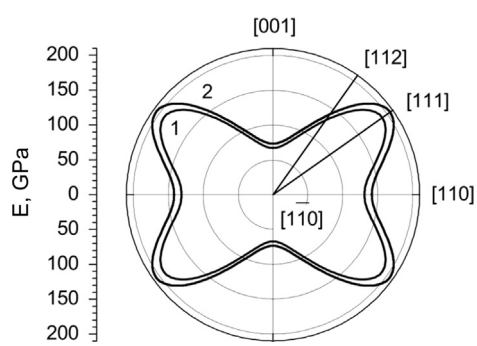

Fig. 9. Sections of the copper Young's modulus characteristic surfaces by the (1$\bar{1}$0) plane at 300 K (line 1) and 5 K (line 2).

much less than the characteristic sample dimensions) and the grain orientations are randomly distributed, its elastic properties may be considered as properties of a macroscopically quasi-isotropic medium and can be characterized with the help of the effective elastic coefficients. A few approaches to a description of elastic properties of the quasi-isotropic polycrystals were suggested. Voigt obtained the estimation of the effective elastic moduli under the assumption of homogeneity of deformations in the polycrystal. Reuss made averaging of compliance coefficients assuming homogeneity of stress distribution (see, for example, [15]). Hill [16] showed that the Voigt and Reuss averages determine, in fact, the upper and lower boundaries for the elastic moduli of quasi-isotropic polycrystals. He suggested using for estimations of the effective moduli the arithmetic (or geometric) mean of the Voigt and Reuss results. The Young's modulus of the quasi-isotropic cubic polycrystal under the assumptions of Voigt (E_V), Reuss (E_R) and Hill (E^A_{VRH}, E^G_{VRH}) may be expressed through the single crystal elastic constants as

$$E_V = \frac{(C_{11}+2C_{12})(C_{11}-C_{12}+3C_{44})}{2C_{11}+3C_{12}+C_{44}}, \tag{2}$$

$$E_R = \frac{5C_{44}(C_{11}+2C_{12})(C_{11}-C_{12})}{C_{11}(C_{11}+3C_{44})+C_{12}(C_{11}-2C_{12}+C_{44})}, \tag{3}$$

$$E^A_{VRH} = \frac{E_V+E_R}{2}; \quad E^G_{VRH} = \sqrt{E_V E_R}. \tag{4a, b}$$

In Table 2, experimental and calculated under Eqs. (2)–(4) values of the Young's modulus of the copper polycrystal at 5, 77 and 300 K are collected. It can be seen that the measured after SPD values of E are higher than the upper boundary given for the quasi-isotropic polycrystals by the Voigt approximation, Eq. (2). At the same time, in the samples annealed at temperatures $T_{ann} \geq 370$ °C the Young's modulus falls to the values that lie well below those obtained by the Reuss averaging.

The results obtained show that the used scheme of SPD-processing leads to a formation in the samples of a structure with pronounced anisotropic properties. Annealing of the samples does not lead to the restoration of a quasi-isotropic state but, per contra, promotes some transition into another anisotropic state with very low values of the Young's modulus.

Anisotropy of the elastic properties of the polycrystalline samples may be caused by the formation of some kind of a crystallographic texture. An analysis of the results obtained allows us to suppose that the most probable mechanisms of the significant changes of the Young's modulus at the various technological stages of the sample processing may be as follows:

(1) formation of the pronounced ⟨111⟩ axial crystallographic texture as a result of heavy plastic deformation according to the SPD scheme used;
(2) transformation of the ⟨111⟩ texture dominating after deformation into the ⟨001⟩ axial texture that becomes prevalent for annealing temperatures above 360 °C;
(3) formation of the final crystallographic annealing ⟨112⟩ texture and/or of the quasi-isotropic polycrystalline state; it should be noted, that the values of the Young's modulus $E^{\langle 112\rangle} \approx E_{CGFA}$, i.e., of these two states are practically indistinguishable for the experimental investigation of the Young's modulus of copper.

Table 2
Young's modulus measured in the ultrafine-grained fire refined tough pitch (UFG FRTP) copper wire at 5, 77 and 300 K as well as elastic stiffnesses C_{11}, C_{12}, C_{44} and values E_V, E_R, E^A_{VRH}, E^G_{VRH} calculated from Eqs. (2)–(4).

T, (K)		5	77	300
$E_{as\ prepared}$, (GPa)		166.83	164.88	154.09
E_{ann}, (GPa)	150 °C	167.45	166.06	155.60
	290 °C	161.10	159.86	149.76
	330 °C	149.97	148.64	138.96
	350 °C	135.05	133.92	124.84
	370 °C	108.06	106.83	99.01
	410 °C	90.40	89.41	82.46
	470 °C	94.72	93.78	86.70
C_{11}, (GPa) ([10,17])		176.58	175.63	169.6
C_{12}, (GPa) ([10,17])		124.8	124.31	122.4
C_{44}, (GPa) ([10,17])		81.4	80.65	75.4
E_V, (GPa)		155.93	154.59	144.92
E_R, (GPa)		119.20	118.18	109.81
E^A_{VRH}, (GPa)		137.57	136.38	127.36
E^G_{VRH}, (GPa)		136.33	135.16	126.15

These assumptions agree rather well with the results of a texture analysis of the MC ETP copper wires deformed by drawing. It has been established that a zoned textural state is observed in samples after drawing. The wire may be regarded as a composite material in which the central zone represents interlacing of fibers having ⟨001⟩ and ⟨111⟩ orientations along the wire axis. In the peripheral zone, the orientations close to the ⟨112⟩ direction are dominating. During annealing, the zoned texture is kept in the wires but the proportion between volume fractions of ⟨111⟩ and ⟨001⟩ orientations in the central zone radically changes and after annealing at the temperatures $T_{ann} > 350$ °C the ⟨001⟩ axial texture becomes dominating in the central zone of the samples.

An analytical description of the elastic properties of the polycrystals with a crystallographic texture is much more difficult than that for the quasi-isotropic case. To account for the anisotropy, the orientation distribution function (ODF) $f(\alpha,\beta,\gamma)$ (α, β, γ are the Euler angles) should be taken into consideration. ODF describes distribution of the crystal grains orientations with respect to one (uniaxial texture), two or three chosen directions in the sample. ODF may be represented either by a discrete distribution of orientations or by a continuous one. From the data on ODF, the elastic coefficients of a textured material are obtained as [15]

$$\langle C_{ijkl}\rangle = \frac{1}{8\pi^2}\int_0^{2\pi}\int_0^{\pi}\int_0^{2\pi} C_{ijkl}(\alpha,\beta,\gamma) f(\alpha,\beta,\gamma)\sin\beta\, d\alpha\, d\beta\, d\gamma. \quad (5)$$

To use Eq. (5) for the calculation of the average values of the elastic constants, one should have experimentally defined ODF for all structural states of the material investigated. However, in some cases one can to make a semi-quantitative estimation, considering ODF as a discrete set of the orientations prevailing in the sample given. In particular, it can be applied to the samples investigated in the present work. As it was mentioned above, deformed samples can be regarded as a composite material consisting of fibers with different orientations along the drawing axis (see also [18]). In all our experiments, the Young's modulus was also measured in this direction. For simplicity, we can assume that the volume of the sample consists of three states of a material: with the ⟨111⟩ texture, with the ⟨001⟩ texture and some peripheral zone in which both the ⟨112⟩ orientation and/or the quasi-isotropic polycrystalline state are observed (in the peripheral zone the Young's modulus value is close to E_{CGFA}).

If m is the volume fraction of the peripheral zone and $E(T_{ann})$ is the value of Young's modulus measured after annealing at T_{ann}, the volume fraction $n^{\langle 111\rangle}$ occupied by the ⟨111⟩ texture may be obtained as

$$n^{\langle 111\rangle} = \frac{E - mE_{CGFA} - (1-m)E^{\langle 001\rangle}}{E^{\langle 111\rangle} - E^{\langle 001\rangle}}. \quad (6)$$

Calculations made according to Eq. (6) show that after the deformation the ⟨111⟩ and ⟨001⟩ textures occupy about 62% and 18% of the sample volume, respectively. After annealing of the samples at 410 °C, these fractions change to 3.2% and 76.8% (in both cases, it is assumed that the peripheral zone occupies about 20% of the sample volume).

5. Summary

It is established that the behavior of the elastic characteristics of the ultrafine-grained (UFG) copper samples obtained by two different severe plastic deformation (SPD) methods is essentially different. In contrast to the ECAP processed UFG copper, in the samples prepared by repeated hydrostatic extrusion and drawing the significant (up to 20%) **increase** in the Young's modulus as compared with that in the well annealed coarse-grained Cu samples is revealed.

Isothermal annealing at temperatures up to 150 °C leads to an additional slight (less than 1%) growth of the Young's modulus. This increase of E is caused mainly by an essential decrease of the dislocation density in the samples. After annealing at higher temperatures, the Young's modulus falls down to values 35% smaller than those in the well annealed coarse-grained samples.

Comparison of the results obtained on the UFG fire refined tough pitch (FRTP) copper with the data of the texture analysis made for the microcrystalline electrolytic tough pitch (MC ETP) copper shows that abnormally high values of the Young's modulus in the SPD-deformed samples are due to the prevalence of the ⟨111⟩ crystallographic axial texture having the highest Young's modulus in copper. A significant reduction of the Young's modulus when annealing at elevated temperatures is caused by the replacement of the ⟨111⟩ axial texture by the ⟨001⟩ one.

Acknowledgments.

We are grateful to Dr. S.N. Smirnov for useful comments and to Dr. L.F. Sennikova for assistance with experiments.

References

[1] Y. Estrin, A. Vinogradov, Acta Mater. 61 (2013) 782–817.
[2] Y.A. Burenkov, S.P. Nikanorov, B.I. Smirnov, V.I. Kopylov, Phys. Solid State 45 (2003) 2119–2123.
[3] N. Kobelev, E. Kolyvanov, Y. Estrin, Acta Mater. 56 (2008) 1473–1481.
[4] E.N. Vatazhuk, P.P. Pal-Val, L.N. Pal-Val, V.D. Natsik, M.A. Tikhonovsky, A.A. Kupriyanov, Low Temp. Phys. 35 (2009) 417–423.
[5] I.S. Golovin, Y. Estrin, Mater. Sci. Forum 667–669 (2011) 857–862.
[6] I.S. Golovin, P.P. Pal-Val, L.N. Pal-Val, E.N. Vatazhuk, Y. Estrin, Solid State Phenom. 184 (2012) 289–294.
[7] P.P. Pal-Val, L.N. Pal-Val, Met. Sci. Heat Treat. 54 (2012) 234–238.
[8] V.D. Natsik, E.N. Vatazhuk, P.P. Pal-Val, L.N. Pal-Val, V.A. Moskalenko, Low Temp. Phys. 39 (2013) 1078–1089.
[9] V.D. Natsik, P.P. Pal-Val, S.N. Smirnov, Acoust. Phys. 44 (1998) 553–560.
[10] H.M. Ledbetter, Phys. Stat. Sol. (a) 66 (1981) 477–484.
[11] F.F. Kraft, U. Chakkingal, G. Baker, R.N.T. Wright, J. Mater. Process. Technol. 60 (1–4) (1996) 171–178.
[12] Yu.N. Loginov, P.A. Vasilevski, L.V. Radionov, Non-Ferrous Met. 6 (2004) 104–106 (in Russian).
[13] S. Jakani, T. Baudinb, C.-H. de Noviona, M.-H. Mathon, Mater. Sci. Eng. A 456 (2007) 261–269.
[14] L.D. Landau, E.M. Lifshitz, Theory of Elasticity, Pergamon Press, Oxford (1970) 43.
[15] T.D. Shermergor, Theory of Elasticity of Micro-Inhomogeneous Media, Nauka, Moscow, 1977.
[16] R. Hill, Proc. Phys. Soc. A 65 (1952) 349–354.
[17] H.M. Ledbetter, E.R. Naimon, J. Phys. Chem. Ref. Data 3 (1974) 897–935.
[18] S.L. Demakov, Y.N. Loginov, A.G. Illarionov, M.A. Ivanova, M.S. Karabanalov, Phys. Met. Metallogr. 113 (2012) 681–686.